International Journal of Theoretical Physics, Vol. 36, No. 11, 1997

Calculation of the Large-N Limit of CMB Anisotropies Induced by Global Scalar Fields

Martin Kunz[1] and Ruth Durrer[1]

Received June 25, 1997

Usually large 3D simulations are used to calculate the cosmic microwave background anisotropies induced by global scalar fields. By going to the large N limit and solving the equations of motion analytically, we can drastically reduce the amount of numerical computations needed, while still finding results quite similar to the corresponding functions in the texture model.

1. INTRODUCTION

The anisotropies in the cosmic microwave background (CMB) have become an extremely valuable tool for cosmology. There are hopes that the measurements of the CMB anisotropy spectrum might lead to a determination of cosmological parameters like Ω_0, H_0, Ω_B, and Λ to within a few percent. The justification of this hope lies in large part in the simplicity of the theoretical analysis. Fluctuations in the CMB can be determined almost fully within linear cosmological perturbation theory and are not severely influenced by nonlinear physics.

There are two competing classes of models which lead to a Harrison–Zel'dovich spectrum of fluctuations: Perturbations may be induced during an inflationary epoch or they may be due to scaling seeds, e.g., a self-ordering global scalar field or cosmic strings [for a general definition of scaling seeds see Durrer and Sakellariadou (1996)]. In the first class, the linear perturbation equations are homogeneous. In the second class they are inhomogeneous, with a source term due to the seed. The evolution of the seed is in general nonlinear and complicated and therefore much less accurate predictions have been made so far for models where perturbations are induced by seeds.

[1]Université de Genève, Ecole de Physique, CH-1211 Geneva, Switzerland.

0020-7748/97/1100-2489$12.50/0

In this work we discuss an especially simple model with seeds where the equation of motion for the seed perturbations can be solved explicitly. We consider an N-component real scalar field ϕ with $O(N)$ symmetric potential V, which at $T = 0$ is given by $V = \lambda(\phi^2 - \eta^2)^2$. At low temperatures, $T << \eta$, ϕ can be regarded as constrained to an $(N-1)$-sphere with radius η. The scalar field then evolves according to the nonlinear σ-model, which is entirely scale-free. In terms of the dimensionless variable $\beta = \phi/\eta$, we obtain the equation of motion

$$\Box\beta - (\beta \cdot \Box\beta)\beta = 0 \tag{1}$$

with the condition $\beta^2 = 1$. The nonlinearity in this equation, $-(\beta \cdot \Box\beta)\beta = (\partial_\mu\beta \cdot \partial^\mu\beta)\beta$, contains a sum over N components. In the limit $N \to \infty$, this sum can be replaced by an ensemble average and the resulting linear equation of motion can be solved exactly. One finds (Turok and Spergel, 1991)

$$\beta(\mathbf{k}, t) = \sqrt{A}t^{3/2}\frac{J_\nu(kt)}{(kt)^\nu}\beta_{in}(\mathbf{k}) \tag{2}$$

The index ν is determined by the background matter model and varies between $\nu = 2$ in a radiation-dominated background and $\nu = 3$ in a matter-dominated background. The prefactor A is chosen to ensure $\beta^2 = 1$,

$$\sqrt{A} = \begin{cases} 8/t_{in}^{3/2} & \text{if } \nu = 2 \\ 48/t_{in}^{3/2} & \text{if } \nu = 3 \end{cases}$$

The components of β_{in} are assumed to be independent, Gaussian-distributed random variables with vanishing mean and dispersion $\langle(\beta_{in})_j^2\rangle = 1/N$ for all values of j. [Clearly, the variables $(\beta_{in})_j$ cannot be completely independent, since they obey the condition $\Sigma_j(\beta_{in})_j^2 = 1$.]

Once the scalar field β is known, we can calculate its energy-momentum tensor, the induced gravitational field, and its action on matter and radiation within linear cosmological perturbation theory. As has been discussed in Turok and Spergel (1991), the energy density of a four-component global scalar field is already quite close to the large-N limit and there are thus justified hopes that this simple model might provide a quite sensible approximation to the texture scenario for structure formation. On the other hand, we know that nonlinearities, which lead to the mixing of scales and to the deviations from a Gaussian distribution, are crucial for some qualitative properties of defect models, like decoherence (Magueijo *et al.*, 1996; Durrer and Sakellariadou, 1996). In the large-N limit, the only nonlinearities are the quadratic expressions of the energy-momentum tensor, and thus effects like decoherence might be weakened substantially in this model.

2. CMB ANISOTROPIES IN MODELS WITH SEEDS

The coefficients of the angular power spectrum of CMB anisotropies are related to the 2-point function by the equation (Padmanabhan, 1993)

$$\left\langle \frac{\delta T}{T}(\mathbf{n}) \frac{\delta T}{T}(\mathbf{n}') \right\rangle \Big|_{(\mathbf{n}\cdot\mathbf{n}'=\cos\varphi)} = \frac{1}{4\pi} \sum_{\ell} (2\ell + 1) C_\ell P_\ell(\cos\theta) \tag{3}$$

For pure scalar perturbations, neglecting Silk damping, the C_ℓ are given by (Durrer and Sakellariadou, 1996)

$$C_\ell = \frac{2}{\pi} \int \frac{\left\langle \left| \Delta_\ell(\mathbf{k}) \right|^2 \right\rangle}{(2\ell + 1)^2} k^2 \, dk \tag{4}$$

where

$$\frac{\Delta_\ell}{2\ell + 1} = \frac{1}{4} \Delta_{gr}(\mathbf{k}, t_{\text{dec}}) j_\ell(kt_0) - V_r(\mathbf{k}, t_{\text{dec}}) \, j'_\ell(kt_0) + k \int_{t_{\text{dec}}}^{t_0} (\Psi - \Phi)(\mathbf{k}, t') j'_\ell(k(t_0 - t')) \, dt' \tag{5}$$

For large ℓ this spectrum is corrected by Silk damping, which can be approximated by multiplying $\Delta_\ell(k)$ with an exponential damping envelope (Hu and Sugiyama, 1996).

We want to consider the situation where fluctuations are induced by seeds. We restrict ourselves to scalar perturbations. The energy-momentum tensor of scalar seed perturbations can be parametrized by the following four functions: f_ρ, the energy density of the seed; f_p, the pressure of the seed; f_v, a potential for the energy flux of the seed; and f_π, the potential for anisotropic stresses of the seed (Durrer, 1990, 1994) (see below). The linear cosmological perturbation equations are then of the form

$$\mathcal{D} X_j = M_j^i F_i \tag{6}$$

where $\mathcal{D}$ is a first-order linear differential operator, X is a vector consisting of all, say m, gauge-invariant perturbation variables of the cosmic fluids (like Δ_{gr}, V_r, and, e.g., the corresponding variables for the cold dark matter (CDM), ...). $F = (f_\rho, f_p, f_v, f_\pi)$ is the source vector and M is an, in general time-dependent, $m \times 4$ matrix.

The general solution to equation (6) is of the form

$$X_j(t) = \int_{t_{in}}^{t} G_j^i(t, t') F_i(t') \, dt' \tag{7}$$

where G is the Green's function of the differential operator $\mathcal{D}$. The Bardeen potentials Φ and Ψ are algebraic combinations of the fluid variables X_j and the source functions F_i,

$$(\Psi - \Phi)(t) = P^j(t)X_j(t) + Q^i(t)F_i(t) \tag{8}$$

Inserting this solution in (5), we obtain

$$\frac{\Delta_\ell}{2\ell + 1} = \int_{t_{in}}^{t_{dec}} dt \left[\frac{1}{4} G^i_{\Delta_r}(t_{dec}, t) j_\ell(kt_0) - G^i_{V_r}(t_{dec}, t) j'_\ell(kt_0)\right] F_i(t)$$

$$+ k \int_{t_{dec}}^{t_0} dt \left[\int_{t_{in}}^{t} dt' (P^j(t) G^i_j(t, t') F_i(t')) + Q^i(t) F_i(t)\right] \tag{9}$$

To calculate the C_ℓ we therefore need to know the unequal time correlations of the seed functions F_i and the Green's functions for the cosmological model specified. In general this is a quite formidable task. Here we shall just discuss a toy model. A somewhat more complicated example is given in Magueijo *et al.* (1996).

We consider a pure radiation universe with vanishing spatial curvature. In this case, the linear perturbation equations are given by (Durrer, 1994)

$$\Phi = \frac{1}{x^2 + 6}\left(x^2\Phi_S + \frac{3}{2}\Delta_{gr} + 6\frac{V_r}{x}\right) \tag{10}$$

$$\Psi = -\Phi - 2\epsilon f_\pi \tag{11}$$

$$\Delta'_{gr} = -\frac{4}{3} V_r \tag{12}$$

$$V'_r = \Psi - \Phi + \frac{1}{4}\Delta_{gr} \tag{13}$$

where $x = kt$ and a prime denotes a derivative with respect to x. The energy-momentum tensor of the source enters via the combinations f_π and $\Phi_S = \epsilon(f_p/k^2 + 3f_v/(kx))$. These equations can be combined to a second-order differential equation for Δ_{gr} alone,

$$\Delta''_{gr} + \frac{12}{x^2 + 6}\frac{\Delta'_{gr}}{x} + \frac{1}{3}\frac{x^2 - 6}{x^2 + 6}\Delta_{gr} = \frac{8}{3}\left(\epsilon f_\pi + \frac{x^2}{x^2 + 6}\Phi_S\right) \tag{14}$$

with homogeneous solutions

$$D_1(x) = \cos\left(\frac{x}{\sqrt{3}}\right) - 2\frac{\sqrt{3}}{x}\sin\left(\frac{x}{\sqrt{3}}\right)$$

$$D_2(x) = -\sin\left(\frac{x}{\sqrt{3}}\right) - 2\frac{\sqrt{3}}{x}\cos\left(\frac{x}{\sqrt{3}}\right)$$

leading to the Green's function

$$G(x, x') = \frac{\sqrt{3}x'}{x(6 + x'^2)}\left[(12 + xx')\sin\left(\frac{x - x'}{\sqrt{3}}\right)\right.$$
$$\left. + 2\sqrt{3}(-x + x')\cos\left(\frac{x - x'}{\sqrt{3}}\right)\right] \tag{15}$$

On superhorizon scales ($x << 1$) the solutions of the homogeneous equations consist of one constant and one decaying, $\propto 1/x$, mode, while for $x >> 1$ we obtain two oscillating modes. The general solution with source term $S(x)$ and initial condition $\Delta_{gr}(0) = V_r(0) = 0$ is

$$\Delta_{gr}(x) = \int_0^x G^1(x, x')S(x')\,dx' \tag{16}$$

$$V_r(x) = \int_0^x G^2(x, x')S(x')\,dx' \tag{17}$$

where

$$G^1 = G \qquad \text{and} \qquad G^2 = -\frac{3}{4}\frac{dG}{dx} \tag{18}$$

3. SCALAR SEED FUNCTIONS IN THE LARGE-N LIMIT

Let us discuss the source correlation functions of scalar field sources in the large-N limit. The seed functions are given by (Durrer, 1994)

$$f_\rho = F_1 = \frac{1}{2}[\dot{\beta}^2 + (\nabla\beta)^2] \tag{19}$$

$$f_p = F_2 = \frac{1}{2}[\dot{\beta}^2 - \frac{1}{3}(\nabla\beta)^2] \tag{20}$$

$$f_v = F_3 = \Delta^{-1}[\dot{\beta} \cdot \beta_{,j}]^{,j} \tag{21}$$

$$f_\pi = F_4 = \frac{3}{2}\Delta^{-2}[\beta_{,i} \cdot \beta_{,j} - \frac{1}{3}\delta_{ij}(\nabla\beta)^2]^{,ij} \tag{22}$$

Using the fact that the initial fields are uncorrelated and Gaussian-distributed,

$$\langle\beta_i(\mathbf{k})\beta_j(\mathbf{p})\rangle = \frac{C}{N}\delta_{ij}\delta(\mathbf{k} + \mathbf{p}), \qquad C = const. \tag{23}$$

and using the exact solution (2), we find the power spectra and the unequal time correlation functions of the seed variables F_i. Below we give explicit expressions for the power spectra of f_ρ, f_v, and f_π and, as an example, the unequal time correlation function for f_v. These integrals can be evaluated numerically, examples of which are shown in Figs. 1 and 2. We define $\mathbf{x} = t\mathbf{k}$ and we set

$$\chi(x) \equiv \frac{J_\nu(x)}{x^\nu}, \qquad \varphi(x) \equiv \frac{3}{2}\frac{J_\nu(x)}{x^\nu} - \frac{J_{\nu+1}(x)}{x^{\nu-1}} \tag{24}$$

Using these abbreviations, we obtain the somewhat cumbersome expressions

$$\dot{\beta}^2(\mathbf{k}, t) = At \int d^3q \varphi(qt)\varphi(|\mathbf{k} - \mathbf{q}|t)\beta_{in}(\mathbf{q})\beta_{in}(\mathbf{k} - \mathbf{q}) \tag{25}$$

$$(\nabla\beta)^2(\mathbf{k}, t) = -At^3 \int d^3q\, \mathbf{q}(\mathbf{k} - \mathbf{q})\chi(qt)\chi(|\mathbf{k} - \mathbf{q}|t)\beta_{in}(\mathbf{q})\beta_{in}(\mathbf{k} - \mathbf{q}) \tag{26}$$

$$f_v(\mathbf{k}, t) = At^2 \int d^3q \frac{\mathbf{k}(\mathbf{k} - \mathbf{q})}{k^2} \varphi(qt)\chi(|\mathbf{k} - \mathbf{q}|t)\beta_{in}(\mathbf{q})\beta_{in}(\mathbf{k} - \mathbf{q}) \tag{27}$$

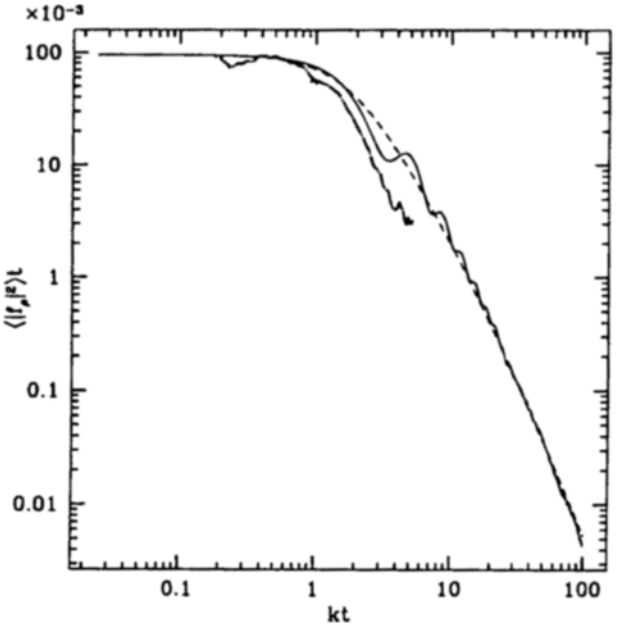

Fig. 1. The source function f_ρ: In the large-N limit (full line), the approximation used to calculate the C_ℓ in Fig. 7 (dashed line) and from a 3-dimensional numerical computation (dot-dashed line) for the texture model ($N = 4$).

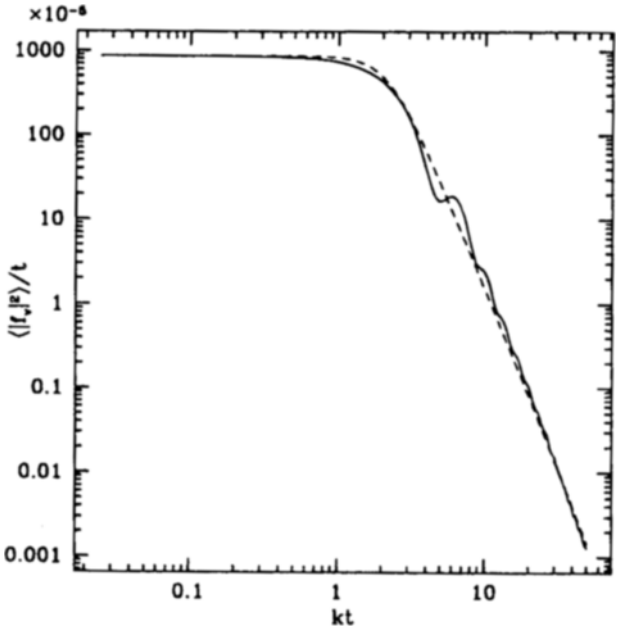

Fig. 2. The source function f_ν: As in Fig. 1, we plot the large-N limit as full line and the approximation as a dashed line.

$$f_\pi(\mathbf{k}, t) = At^3 \int d^3q \, \frac{[(\mathbf{kq})(k^2 - \mathbf{kq}) - \frac{1}{3} k^2 \mathbf{q}(\mathbf{k} - \mathbf{q})]}{k^4} \times \chi(qt)\chi(|\mathbf{k} - \mathbf{q}|t)\beta_{in}(\mathbf{q})\beta_{in}(\mathbf{k} - \mathbf{q}) \tag{28}$$

and some examples for the correlations:

$$\langle f_\rho(\mathbf{k}, t) \cdot f_\rho(\mathbf{k}', t)\rangle = \frac{A^2}{t} \frac{\delta(\mathbf{k} + \mathbf{k}')}{2N} \int d^3y \, \{\varphi(y)^2\varphi(|\mathbf{y} - \mathbf{x}|)^2 + [\mathbf{y}(\mathbf{x} - \mathbf{y})]^2\chi(y)^2\chi(|\mathbf{y} - \mathbf{x}|)^2 - 2\mathbf{y}(\mathbf{x} - \mathbf{y})\varphi(y)\varphi(|\mathbf{y} - \mathbf{x}|)\chi(y)\chi(|\mathbf{y} - \mathbf{x}|)\} \tag{29}$$

$$\langle f_\nu(\mathbf{k}, t) \cdot f_\nu(\mathbf{k}', t)\rangle = A^2 t \frac{\delta(\mathbf{k} + \mathbf{k}')}{N} \int d^3y \, \frac{\mathbf{x}(\mathbf{x} - \mathbf{y})}{\mathbf{x}^4} \varphi(y)\chi(|\mathbf{y} - \mathbf{x}|) \times [\mathbf{x}(\mathbf{x} - \mathbf{y})\varphi(y)\chi(|\mathbf{x} - \mathbf{y}|) + \mathbf{xy}\varphi(|\mathbf{x} - \mathbf{y}|)\chi(y)] \tag{30}$$

$$\langle f_\pi(\mathbf{k}, t) \cdot f_\pi(\mathbf{k}', t)\rangle$$

$$= A^2 t^3 \frac{9\delta(\mathbf{k}+\mathbf{k}')}{2N} \int d^3y \frac{[(\mathbf{xy})(x^2 - \mathbf{xy}) + \frac{1}{3}x^2(y^2 - \mathbf{xy})]^2}{x^8}$$

$$\times \chi(y)^2 \chi(|\mathbf{x} - \mathbf{y}|)^2 \tag{31}$$

$$\langle f_\nu(\mathbf{k}, t) \cdot f_\nu(-\mathbf{k}', t')\rangle$$

$$= \frac{A^2 t}{N}\frac{r^2}{x^4}\delta(\mathbf{k} - \mathbf{k}') \int d^3y \{[x^2 - \mathbf{xy}]^2 \varphi(y)\chi(|\mathbf{x} - \mathbf{y}|)\varphi(yr)\chi(|\mathbf{x} - \mathbf{y}|r)$$

$$+ [(x^2 - \mathbf{xy})(\mathbf{xy})]\varphi(y)\chi(|\mathbf{x} - \mathbf{y}|)\varphi(|\mathbf{x} - \mathbf{y}|r)\chi(yr)\} \tag{32}$$

where we have set $r = t'/t$ in the last equation. The behavior of these functions on very large and very small scales can be obtained analytically. On superhorizon scales, $x \to 0$, the power spectra for f_ρ, f_p, and f_ν behave like white noise. Numerically we have found

$$\langle |f_\rho|^2 \rangle \underset{x\to 0}{\to} \frac{1}{Nt} \cdot \begin{cases} 9.36 \times 10^{-2} & \nu = 2 \\ 10.31 \times 10^{-2} & \nu = 3 \end{cases} \tag{33}$$

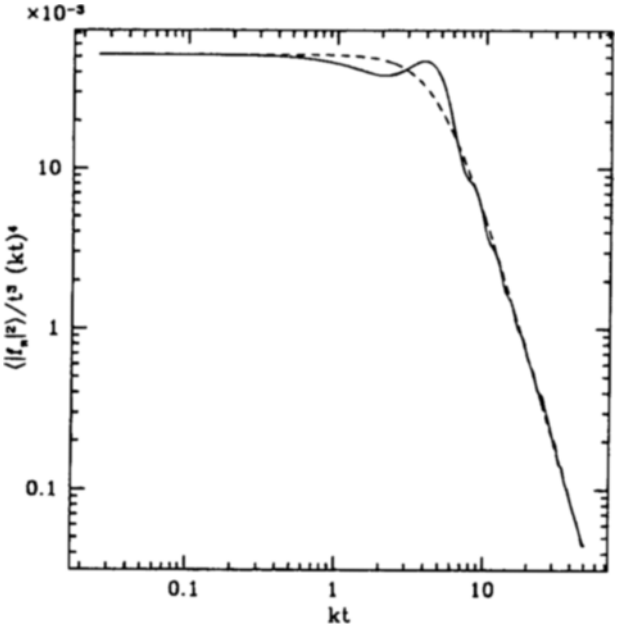

Fig. 3. The source function f_π as in Fig. 2.

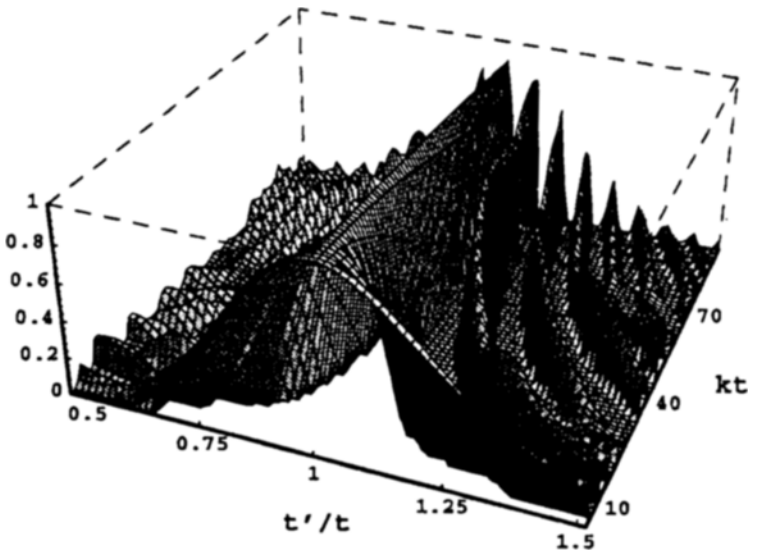

Fig. 4. The unequal time correlation function for $\dot{\beta}^2 = f_\rho + 3f_p$ at fixed t as function of t' and k in the large-N limit. Negative values are set to zero.

$$\langle |f_\rho|^2 \rangle \underset{x\to 0}{\to} \frac{1}{Nt} \cdot \begin{cases} 1.066 \times 10^{-2} & \nu = 2 \\ 0.805 \times 10^{-2} & \nu = 3 \end{cases} \tag{34}$$

$$\langle |f_v|^2 \rangle \underset{x\to 0}{\to} \frac{t}{N} \cdot \begin{cases} 0.8687 \times 10^{-2} & \nu = 2 \\ 0.4694 \times 10^{-2} & \nu = 3 \end{cases} \tag{35}$$

From general arguments (Magueijo *et al.*, 1996; Durrer and Sakellariadou, 1996), superhorizon scales. However, from (31) we find that f_π diverges at small x like $1/x^2$. Even though we do not quite understand this result, it does not lead to divergent Bardeen potentials if we allow for anisotropic stresses in the matter (like, e.g., from a component of massless neutrinos). In this case it can be shown (Durrer and Sakellariadou, 1996) that compensation arranges the anisotropic stresses in the fluid, $p\Pi$ such that $f_\pi + p\Pi \propto x^2 f_\pi$. Therefore, the anisotropic stresses also contribute a white noise component to the Bardeen potentials on superhorizon scales, namely

$$x^4 \langle |f_\pi|^2 \rangle \underset{x\to 0}{\to} \frac{t^3}{N} \cdot \begin{cases} 5.169 \times 10^{-2} & \nu = 2 \\ 6.539 \times 10^{-2} & \nu = 3 \end{cases} \tag{37}$$

In the limit $x \to \infty$ the source functions decay like

$$\langle |f_\rho|^2 \rangle, \langle |f_p|^2 \rangle \underset{x\to\infty}{\to} \frac{x^{1-2\nu}}{Nt} \tag{38}$$

$$\langle |f_v|^2 \rangle \underset{x\to\infty}{\to} \frac{x^{-1-2\nu}t}{N} \tag{39}$$

$$\langle |f_\pi|^2 \rangle \underset{x\to\infty}{\to} \frac{x^{-3-2\nu}t^3}{N} \tag{40}$$

In Fig. 1 we plot $t < |f_\rho|^2 > (x)$ as obtained from (29), and compare it to the corresponding function found by 3D simulations of the texture model. Figures 2 and 3 show $(1/t) < |f_v|^2 > (x)$ and $(x^4/t^3) < |f_\pi|^2(x)$, respectively.

The normalized unequal time correlation functions are defined by

$$C_i(k, t, t') = \frac{\langle f_i(k, t) f_i^*(k, t') \rangle}{\sqrt{\langle |f_i(k, t)|^2 \rangle \langle |f_i(k, t')|^2 \rangle}} \tag{42}$$

In the large-N limit, the correlation functions decay like power laws. For $r \equiv t'/t$ we find in the limit $r >> 1$, $kt' >> 1$ the behavior $C_i \propto r^{-\gamma_i}$, with

$$\gamma_\rho = 3/2, \qquad \gamma_p = 3/2, \qquad \gamma_v = 3/2, \qquad \gamma_\pi = 5/2 \tag{43}$$

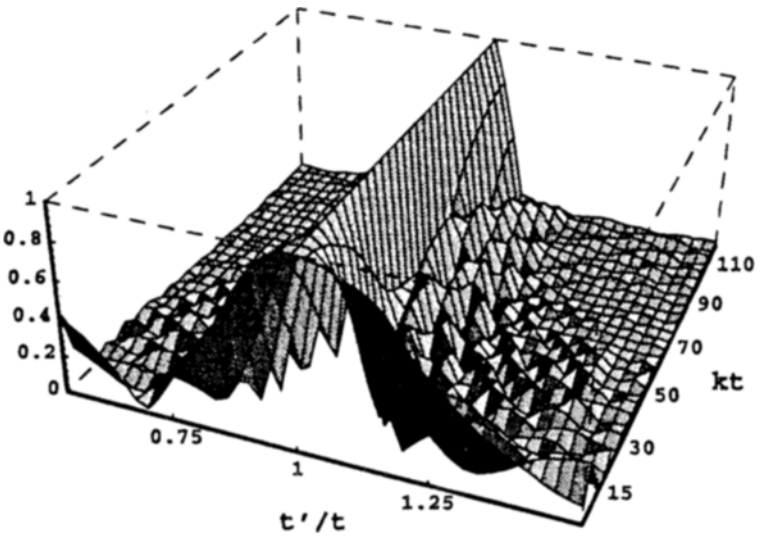

Fig. 5. The same as Fig. 4 for the texture model. The similarity is obvious. The high-order oscillations, which are very pronounced in the large-N limit, are washed out or absent in the texture model. Whether this is a real feature or just numerical inaccuracy or both is not yet clear.

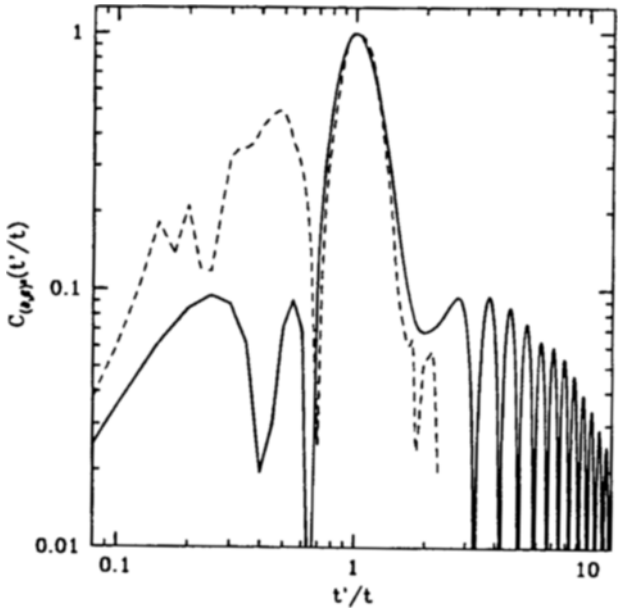

Fig. 6. A cut through Fig. 4 (solid line) and Fig. 5 (dashed line) at $kt = 3.9$. The central peaks are in very good agreement. Secondary peaks do not agree and the decay law for the texture model is difficult to predict from these data.

It is not quite clear to us whether this behavior is reproduced in the texture model. Due to the arguments given at the beginning, it may well be that $N = 4$ and $N \to \infty$ show a different decoherence behavior. Originally (taking into account the numerical accuracy of about 10% of the 3D simulations) we approximated the decoherence in the texture model with an exponential decay law. However, comparing the unequal time correlation functions for β^2 shown in Figs. 4 and 5 for the large-N limit and a 3D simulation of the texture model, respectively, we realize, that they agree extremely well in the numerically most reliable, central region, and the seemingly stochastic higher order oscillations also found in the texture model might actually be real (see Fig. 6), leading to power-law decoherence.

Using these source functions, we have determined the CMB anisotropy spectrum induced by the large-N limit of a self-ordering scalar field for a spatially flat cosmological model with CDM, radiation and baryons. Results are shown in Fig. 7. Since decoherence is so weak for large N, we used the approximation of perfect coherence, $C_i \equiv 1$. This simplification has been used so far for all 'analytic approximations' of $O(N)$ models and, e.g., in the case of textures, $N = 4$, it seems to agree reasonably with numerical simulations (Turok, 1996). This will certainly be even more so in the large-N limit.

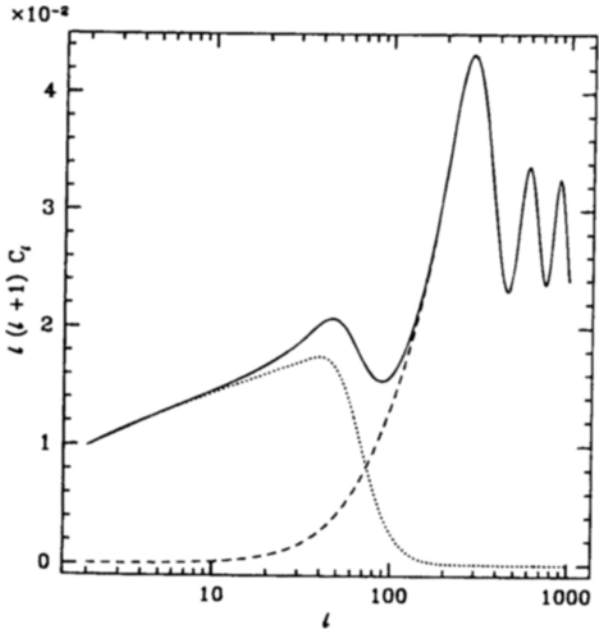

Fig. 7. The CMB anisotropy spectrum, obtained by using polynomial fits for the source functions as shown in Figs. 1–3. Only scalar perturbations are included. The Sachs–Wolfe part is indicated by the dotted line, the dashed line represents the acoustic contributions. Silk damping is not included.

The influence of decoherence on the CMB power spectrum is discussed in Magueijo *et al.* (1996).

4. CONCLUSION

We have shown that the large-N limit of global scalar fields provides a model of seeded structure formation where CMB anisotropies can be determined without cumbersome numerical simulations and thus with much higher accuracy and larger dynamical range at relatively modest costs. Determining the correlation functions of the seed variables just requires numerical convolution of Bessel functions multiplied with powers. Once the seed correlation functions are known, perturbations in matter and radiation can be calculated by solving a system of linear perturbation equations, very similar to the homogeneous case of inflationary perturbations.

We believe that the large-N limit has many features in common with the texture model of structure formation and thus provides a "cheap approximation" to this model. The most obvious difference between the analytic limit and the texture model is the decoherence behavior. In the large-N limit,

the field evolution is linear and nonlinearities, which are responsible for decoherence, enter only via the quadratic expressions of the energy-momentum tensor. We thus expect decoherence to be somewhat weaker in the large-N limit.

In a forthcoming paper, we plan to work out the large-N limit in more detail, and to study the dependence of the resulting CMB anisotropy spectrum of cosmological parameters. We also want to investigate more fully the comparison of the large-N source functions with the source functions found in 3D simulations of the texture model. The limit discussed here provides a very useful toy model for structure formation with scaling seeds for which decoherence is not important.

REFERENCES

Durrer, R. (1990). *Physical Review* D, **42**, 2533.
Durrer, R. (1994). *Fundamentals of Cosmic Physics*, **15**, 209.
Durrer, R., and Sakellariadou, M. (1996). In preparation
Hu, W., and Sugiyama, N. (1996). Small scale cosmological perturbations: An analytic approach, astro-ph/9510117.
Magueijo, J., Albrecht, A., Ferreira, P., and Coulson, D. (1996). Preprint, astro-ph/9605047.
Padmanabhan, T. (1993). *Structure Formation in the Universe*, Cambridge University Press, Cambridge.
Turok, N. (1996). Preprint [astro-ph/9606087].
Turok, N., and Spergel, D. (1991). *Physical Review Letters*, **66**, 3093.